

# Contents

<b>1</b>	<b>Introduction</b>	<b>1</b>
<b>2</b>	<b>Model and Method</b>	<b>3</b>
2.1	Theoretical Model . . . . .	3
2.1.1	Phase Diagram . . . . .	4
2.2	Simulation Method . . . . .	5
2.3	Analysis . . . . .	5
<b>3</b>	<b>Results</b>	<b>7</b>
3.1	Varying the Composition . . . . .	7
3.1.1	Pure Species 2 (two patches, $x = 0$ ) . . . . .	7
3.1.2	Pure Species 1 (three patches, $x = 1$ ) . . . . .	8
3.1.3	Mixtures . . . . .	11
3.2	Varying the Ratio of Buoyant Masses . . . . .	11
3.2.1	Negative Masses . . . . .	11
3.2.2	Positive Masses . . . . .	12
<b>4</b>	<b>Conclusion and Outlook</b>	<b>16</b>
<b>5</b>	<b>References</b>	<b>17</b>
<b>6</b>	<b>APPENDIX A: Implementation Details</b>	<b>18</b>
6.1	Data . . . . .	19
6.2	Analysis tools . . . . .	19

## **Abstract**

We investigate the stacking sequences of a two-dimensional binary mixture of patchy colloids in sedimentation-diffusion equilibrium using Monte Carlo simulation. The examined system consists of a mixture of colloids with two and three bonding sites (patches) in a vessel with hard walls. The parameters of the simulation include the ratio of buoyant masses of the two species, the gravitational length, the temperature, and the composition.

We could reproduce the theoretically predicted stacking sequences for different relative buoyant masses and compositions. We found unexpected behaviour for high relative buoyant masses.

# 1 Introduction

The examination of colloids with bonding sites (known as patchy colloids) has revealed many interesting phenomena. Bianchi et al. first studied a three-dimensional system of patchy colloids [1] that behaves as an empty liquid: A liquid that coexists with a vapor phase at vanishing packing fraction (and thus a vanishing density). Russo et al. later studied the two-dimensional case of a binary mixture of colloidal disks with three (species 1  ) and two (species 2  ) bonding sites [2] and found the same behaviour.

Sedimentation, as opposed to the study of a bulk, allows the exploration of the phase diagram in lines instead of points. Where a simulation of a bulk system (e.g. with periodic boundary conditions) has one equilibrium state at a point in the phase diagram, a simulation in a box with gravity has a varying external energy as a function of height and thus creates a path through the phase diagram. This can result in multiple coexisting phases stacked on top of each other: A stacking sequence. D. de las Heras and M. Schmidt have, for example, found a rich landscape of stacking sequences for colloidal mixtures [3].

We want to combine the rich phenomenology of patchy colloidal systems with the possibility to observe coexisting phases. We take the system studied by Russo et al. [2] and subject it to a gravitational field to study sedimentation.

We choose the following dimensionless parameters (see table 1 for an overview) for our study:  $T^*$  is the ratio of thermal energy  $k_B T$  (where  $T$  is the temperature and  $k_B$  the Boltzmann constant) and the energy of one bond ( $U_0$ , see chapter 2.1 for details). It controls how easily bonds are broken.  $G$  is the ratio of gravitational energy  $m_1 g \sigma$  (where  $\sigma$  is the diameter of a colloid,  $g$  is the gravitational acceleration and  $m_1$  the buoyant mass of one particle of species 1  ) and, again, bonding energy.  $M$  is the ratio of the buoyant masses of the species.  $x$  denotes the composition of the mixture, namely the molar fraction of species 1  .

In our study, we first reproduce Russo's bulk phase diagram (Figure 10 of Ref. [2]) in a temperature range of  $T^* = 0.2$  to  $0.05$ . While Russo et al. used a Virtual Move Monte Carlo (VMMC) scheme [4], we use a simpler one that only moves a single particle at a time. While this results in low acceptance rates, we found that it is sufficient to reproduce the previously reported behaviour for temperatures  $T^* \gtrsim 0.05$ .

We then consider a gravitational field that adds a contribution to the external energy of each particle, according to the respective buoyant mass. We confine the particles in a vessel with hard walls. The presence of a background medium for the particles causes a buoyant mass that can be negative as well as positive. Species 1  sets the unit of mass.  $G$  is set so that for species 1  , the gravitational length  $\frac{L}{\sigma} = \frac{T^*}{G}$  is similar to the height of the simulation vessel. For the current purposes,  $G = 0.005$  proved to be suitable.

Our main interest concerns the effect of mass and composition on the stacking sequence in the vessel. We study these parameters for a temperature of  $T^* = 0.15$ . This temperature allows for a high mobility of the particles while being low enough such that bonds and networks still form. For temperatures of 0.2 and above, network formation is not observed, while temperatures of 0.1 or lower require exceedingly long simulation times.

## 1 Introduction

---

We expect to see stacking sequences with up to three distinct phases as predicted by Wertheim theory (see e.g. [5]).

Table 1: Dimensionless Parameters used in the simulation.  $\sigma$  denotes the Diameter of a colloid,  $T$  the temperature,  $k_B$  the Boltzmann constant,  $U_0$  the energy of a bond (see chapter 2.1),  $g$  the gravitational acceleration,  $m_i$  the buoyant mass of species  $i$  and  $N_i$  the number of particles of species  $i$ .

Description	Symbol	Definition	Min. Value	Max. Value
Ratio of thermal & interaction energy	$T^*$	$\frac{k_B T}{U_0}$	0.05	1.0
Ratio of gravitational energy scale & interaction energy	$G$	$\frac{m_1 g \sigma}{U_0}$	0.001	0.01
Ratio of buoyant masses	$M$	$\frac{m_2}{m_1}$	-3	6
Composition (molar fraction of species 1)	$x$	$\frac{N_1}{N_1 + N_2}$	0.0	1.0

## 2 Model and Method

### 2.1 Theoretical Model

We consider a binary mixture of patchy colloids in two dimensions. Each particle consists of a hard disk core with diameter  $\sigma$  which sets the unit of length. Hard disk interactions imply that any two disks cannot overlap. Bonding sites are located on the surface of each colloid. Each bonding site is modelled as a disk of diameter  $\delta = \frac{\sqrt{5-2\sqrt{3}}-1}{2}\sigma$ . This value is „the largest value which guarantees that each site is engaged at most in one bond“[2]. The centre of each bonding site is located on the surface of the colloid. We consider two species, one of which has three patches and is referred to as species 1  $\blacktriangle$ . Species 2  $\blacksquare$  has two patches. The exact positions of the patches are given in figure 1. When the bonding sites of two colloids overlap, which means that the centre of any bonding site on particle  $A$  has a distance of  $\delta$  or less from the centre of any bonding site on particle  $B$ , a bond of bonding energy  $U_0$  is formed. Hence the patches interact via a square-well interaction. Thus, we get three coordinates for each particle  $i$ : The positions  $x_i$  and  $z_i$  of its centre as well as an angle  $\alpha_i$  to define the position of the patches as shown in figure 1.

For initial testing and reproduction of Russo et al.’s results, we consider a system without external energy and with periodic boundary conditions. Our main interest being sedimentation, we then implement an external gravitational potential

$$V_g := \sum_{i=0}^N m_i g z_i \quad (1)$$

as well as a vessel with hard walls. We fix the mass of species 1  $\blacktriangle$  particles as the unit of mass and vary the relative mass of species 2  $\blacksquare$  particles (see table 1). To see the effects of gravity, we choose the gravitational length ( $\frac{L}{\sigma} = \frac{T^*}{G}$ ) to be similar to the height of the simulation vessel. We set the ratio of gravitational energy  $m_1\sigma$  and interaction energy to 0.005 to achieve this, the geometry of the vessel being  $100\sigma$  (width) by  $200\sigma$  (height).

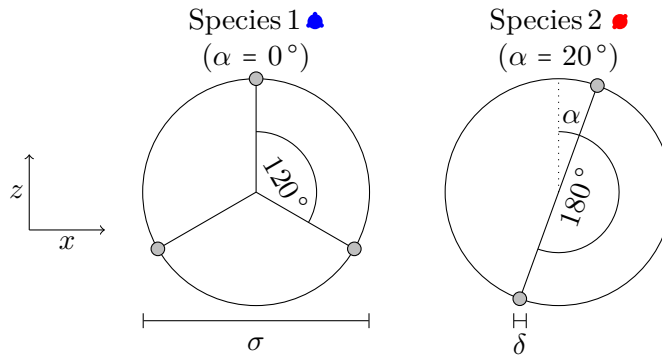


Figure 1: Sketch of the geometry of the patchy colloids. Species 1 (left) has three bonding sites, species 2 has two bonding sites. The angle  $\alpha_i$  denotes the rotation of particle  $i$ .

## 2 Model and Method

---

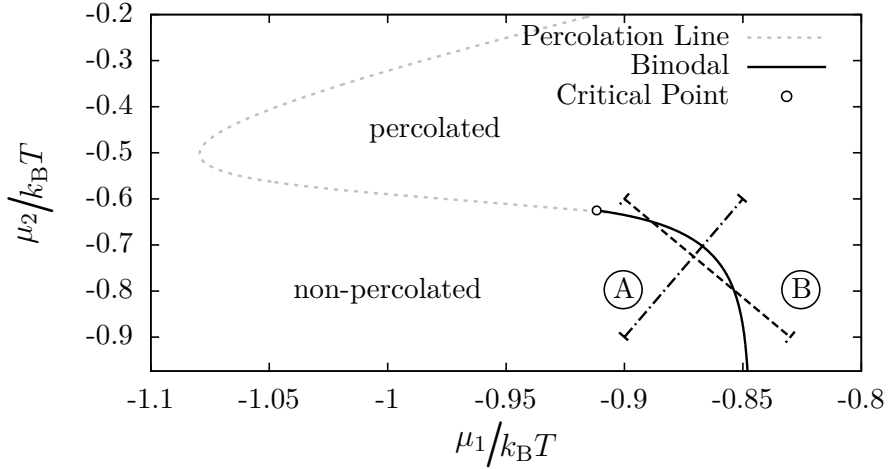


Figure 2: Phase diagram in the plane of chemical potentials at  $T^* = 0.1$  of a binary mixture of hard disks with two or three patches according to Wertheim's theory.  $\mu_i$  is the chemical potential for species  $i$ . Path  $A$  and  $B$  are examples of sedimentation paths. The direction (which end corresponds to the bottom of the box) is controlled by the sign of the buoyant masses  $m_1, m_2$ . The number of phases is  $1 + n_{\text{cross}}$  where  $n_{\text{cross}}$  is the number of times the path crosses the binodal.

### 2.1.1 Phase Diagram

Figure 2 shows results by Daniel de las Heras [6] for the phase diagram of our system in the plane of chemical potentials<sup>1</sup>. The binodal separates a high-density 'liquid' phase (above the binodal) from a low-density 'vapour' phase. The percolation line separates a percolated state from a non-percolated state.

We know that the difference in chemical potential between two points for a given species is the difference in gravitational energy [7]. Therefore, if we plot  $(\mu_1, \mu_2)$  as a function of height  $z$ , we will get a straight line (sedimentation path) through the  $\mu_1, \mu_2$  plane. Moreover, we can control the slope of the sedimentation path by the ratio of buoyant masses. If  $M$  is negative (positive), the path will have a negative (positive) slope. It should therefore be possible to get multiple phase sequences in the simulated system (see figure 2).

Because we do not have information about the value of the chemical potential in the simulation (this could be implemented in principle by Widom's test particle insertion method [8]), we can just control the slope and length of the path, but not its position in the plane of chemical potentials, so a bit of trial and error is required.

Figure 2 shows two different possible paths through the phase diagram. Path  $A$  crosses the binodal once, resulting in two coexisting phases: One is percolated and the other is not. Path  $B$  crosses it twice, resulting in three phases, two percolated ones with a non-percolated phase in the middle. The sign of the buoyant masses determines which end of the path represents which end of the simulation box. The chemical potential always increases with the effective gravitational energy. Apart from paths crossing the binodal,

<sup>1</sup>It should be noted that the results are only approximate, because the theory assumes a purely tree-like topology of the network formed by the colloids, i.e. closed loops cannot exist

paths crossing the percolation line could also result interesting stacking sequences.

### 2.2 Simulation Method

We use the standard Monte Carlo simulation method via single particle moves to obtain the equilibrium states of the system. This allows for an easier implementation than, for example, VMMC (used by Russo et al. [2]). However temperatures below  $\sim 0.05$  are effectively in-accessible by this approach because of the long simulation times required to reach equilibrium.

The initialisation of the particle coordinates is done randomly while avoiding collisions. We then thermalise the system at a high temperature ( $T^* = 0.5$ ) with zero gravity, running 10000 MC steps. Here, one MC step consists of a trial displacement and trial rotation of each particle. The resulting trial move is accepted with the standard Metropolis acceptance probability depending on the change in total energy  $\Delta E$ . The acceptance probability is  $\exp(-\frac{\Delta E}{T^*})$  if  $\Delta E$  is positive; changes that decrease the energy are always accepted. The displacement in  $x$  and  $z$  is chosen uniformly from the interval  $[-d_{\max}, d_{\max}]$  and the rotation from the interval  $[-\alpha_{\max}, \alpha_{\max}]$ . Details on the limits are given in chapter 6.

### 2.3 Analysis

To analyse the simulation output, we primarily create plots of the final configuration and the density profile. A density profile consists of the number densities in intervals in  $z$  of fixed height.

$$\rho_i = \frac{N_{1,i} + N_{2,i}}{W \cdot \Delta z} \quad (2)$$

In this way, we get an approximation of  $\rho(z)$ , which helps us characterise different phases. From  $\rho$ , we can also calculate the *packing fraction*, which is the fraction of the area in the box covered by colloids. It is related to the (total) number density by a factor of  $\pi \frac{\sigma^2}{2} = \frac{\pi}{4}$ , the area of one colloid. In much the same way, we get a profile of the bond saturation as a function of height. For each interval, we count the number of bonds and the number of possible bonds (half the number of available bonding sites). This gives us an indication as to whether a network has been formed.

$\Delta z$  is the height of the interval,  $W$  is the width of the simulation box, and  $N_{j,i}$  is the number of colloids of species  $j$  in interval  $i$

#### Characterising Percolation

A percolated state is a state in which for (nearly) every pair of particles  $(i, j)$  in the box,  $i$  is connected to  $j$ .  $i$  and  $j$  are *connected* if either there exists an intermediate particle  $\zeta$  so that  $i$  is bonded directly to  $\zeta$  and  $\zeta$  is *connected* to  $j$  or  $i$  is directly bonded to  $j$ . This can be recognised roughly by visual inspection of the plots of the final configuration, but can also be analysed quantitatively with statistical analysis.

One possibility is to investigate the distribution of connected particles as a function of distance (similar to the radial distribution function). The function is calculated by selecting a pivot particle and counting the number of particles  $N_t(r)$  within a distance  $[r, r + dr]$ . We then determine which of those particles are connected to the pivot. Their number is  $N_c(r)$ . The ratio  $N_c/N_t$  gives the value of the distribution at  $r$ . We can calculate

## 2 Model and Method

---

this function up to a cutoff  $r_{\max}$  and then average over all particles. For a percolated state, we expect the function to be near constant, while for non-percolated states, it will decrease quickly and approach zero for large distances.

The second possibility for analysis of percolation is to compare the bonding probability  $P_{\text{bond}}$  to the percolation threshold as found by de las Heras et al. in [6]. Their theory predicts a bond probability

$$P_{\text{perc}} = \frac{xf_1 + (1-x)f_2}{(1-x)f_2(f_2 - 1) + xf_1(f_1 - 1)} \quad (3)$$

as a lower bound for  $P_{\text{bond}}$  for percolated systems (where  $f_i$  is the number of patches for species  $i$  and  $x$  the local composition). So, if we calculate  $P_{\text{bond}}$ , we can decide if a system is percolated or not. This property is defined locally (e.g. as a function of  $z$ ), so we can use it in some cases to differentiate coexisting phases.

Note that the equation depends only on the composition and the functionality (number of patches) of the species. For our system, the equation reduces to  $P_{\text{perc}} = \frac{x+2}{4x+2}$ , the extrema being 1.0 for  $x = 0$  and 0.5 for  $x = 1.0$  (at least half the bonding sites must be engaged in a bond). It follows that a pure system of species 2 (red) cannot percolate.

### Characterising Equilibrium

We use the behaviour of the total energy of the system as a criterion to determine whether or not a given simulation is equilibrated. In equilibrium, the energy of the system is minimal, so  $\frac{\partial E}{\partial t} = 0$ . Keeping in mind that the energy, especially the internal part, can be quite noisy (depending on the temperature), we can decide if equilibrium has been reached by viewing energy plotted against simulation time (see figure 3). Note that, in the canonical ensemble in equilibrium, the width of the energy fluctuations relates to the heat capacity of the system ( $C_V = \frac{\langle E^2 \rangle - \langle E \rangle^2}{k_B T^2}$ )

Another indicator is the total (buoyant) mass density as a function of height. In an equilibrium state, the density must monotonically decrease with height. The only exceptions are near ( $\sim \sigma$ ) the top and bottom walls because of correlation effects due to the hard core interactions.

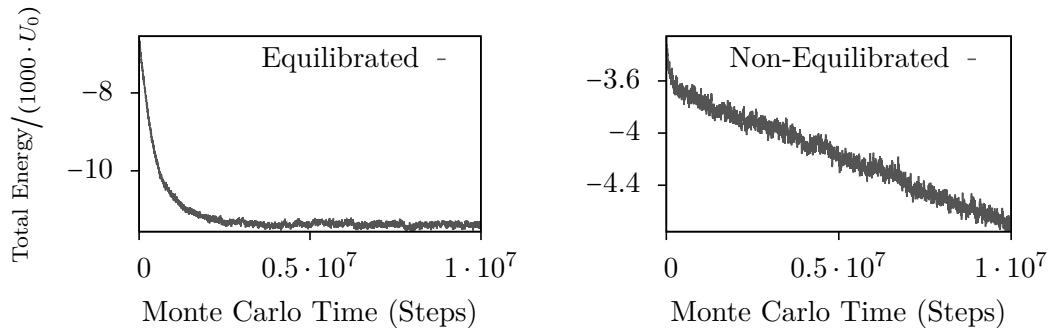


Figure 3: Behaviour of the scaled total energy as a function of Monte Carlo time. Left: An equilibrated system. In equilibrium, the width of the energy fluctuations relates to the heat capacity of the system. Right: System that is not equilibrated yet.

## 3 Results

### 3.1 Varying the Composition

In this case, we choose equal masses for the species ( $m_1 = m_2$ ). The total number of particles is 7500 and we vary the composition in steps of 0.1 from 0 (all species 2 to 1 (all species 1 ). Temperature and gravity are fixed at  $T^* = 0.15, G = 0.005$  and the particles are initialised randomly. The simulation time is  $3 \cdot 10^7$  MC steps, followed by another  $10^7$  steps to get a better sample of the density in equilibrium. We do this to study the different structures arising from different compositions. Because the species have equal masses, the sedimentation path has a positive slope, so the theory predicts two phases at most (see section 2.1.1).

#### 3.1.1 Pure Species 2 (two patches, $x = 0$ )

The bonding sites of species 2 (two bonding sites on opposite sides of the particle) do not allow the formation of a percolated network. Rather, chains of different lengths are formed, longest at the bottom, shortest (up to single particles) on top (see figure 7a). While the density is high at the bottom and low on top, there is no phase transition, since the density changes gradually rather than sharply. Since species 2 cannot percolate, there are no percolated areas. Near the edges of the box we can see that the orientation of the particles is highly influenced by the presence of walls (see figure 4a). For maximum bonding, a line through both patches of a particle must be oriented parallel to the wall (left and bottom in figure 4a). Farther from the walls, no such orientational preference can be observed (e.g. top right corner).

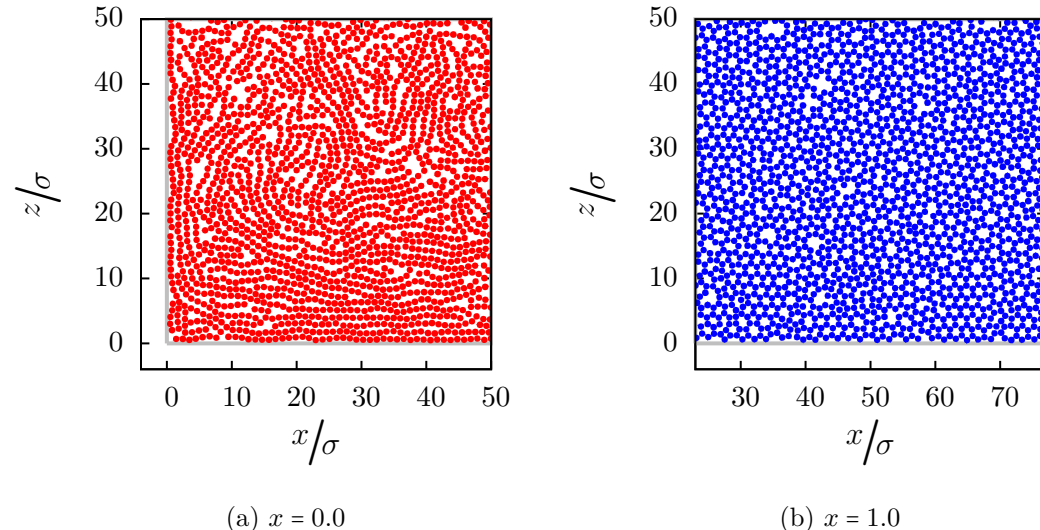


Figure 4: Illustration of typical final configurations for pure systems of species 2 (a) and species 1 (b). Species 2 forms chains and has a high density near the walls (in gray), while species 1 forms a circular mesh with a low density near the walls.

### 3 Results

---

Another noteworthy feature is the density at the wall. The bond geometry allows close proximity to the wall, and we observe an adsorption effect (see figure 5).

#### 3.1.2 Pure Species 1 (three patches, $x = 1$ )

Species 1  shows a completely different structure from species 2 . The preferred configuration is in rings of different sizes, 4 being the lowest possible number of colloids in a ring. This sort of configuration is less dense than for ordered species 2  layers that get close to hexagonal packing (the configuration with the highest possible density for hard disks). On the other hand, it is not dependent on wall effects. Therefore, the density drops much slower as a function of height.

Pure systems of species 1  easily percolate ( $p_{\text{perc}} = 0.5$ , see figure 6j) and form a dense and stable mesh. For high densities, single particles can be trapped inside a ring and have no bonds. The transition to the low-density vapour phase is much sharper than for species 2 .

The bond geometry does not allow these particles to be close to the wall while maximising the number of bonds. Therefore, the density drops at the wall rather than rising, as observed with species 2  (compare figure 5).

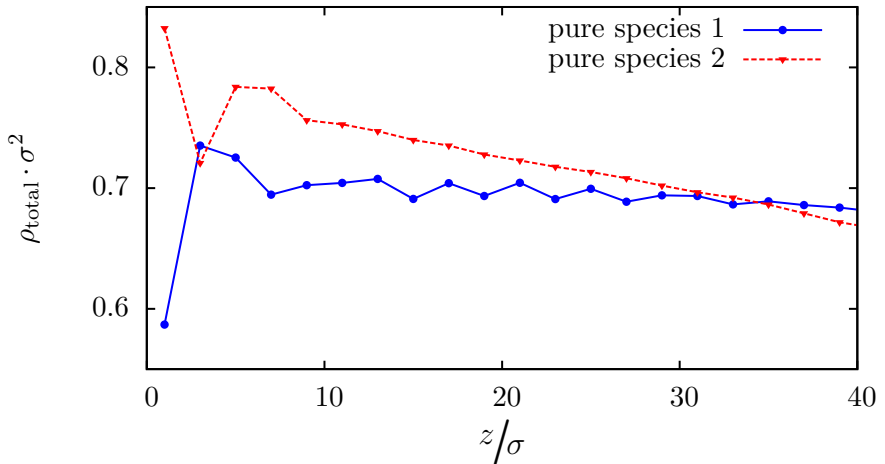


Figure 5: Number density for pure systems of species 1 and 2 near the bottom wall (lines are a guide to the eye). Species 2 is adsorbed to the wall, while species 1 is repelled.

### 3 Results

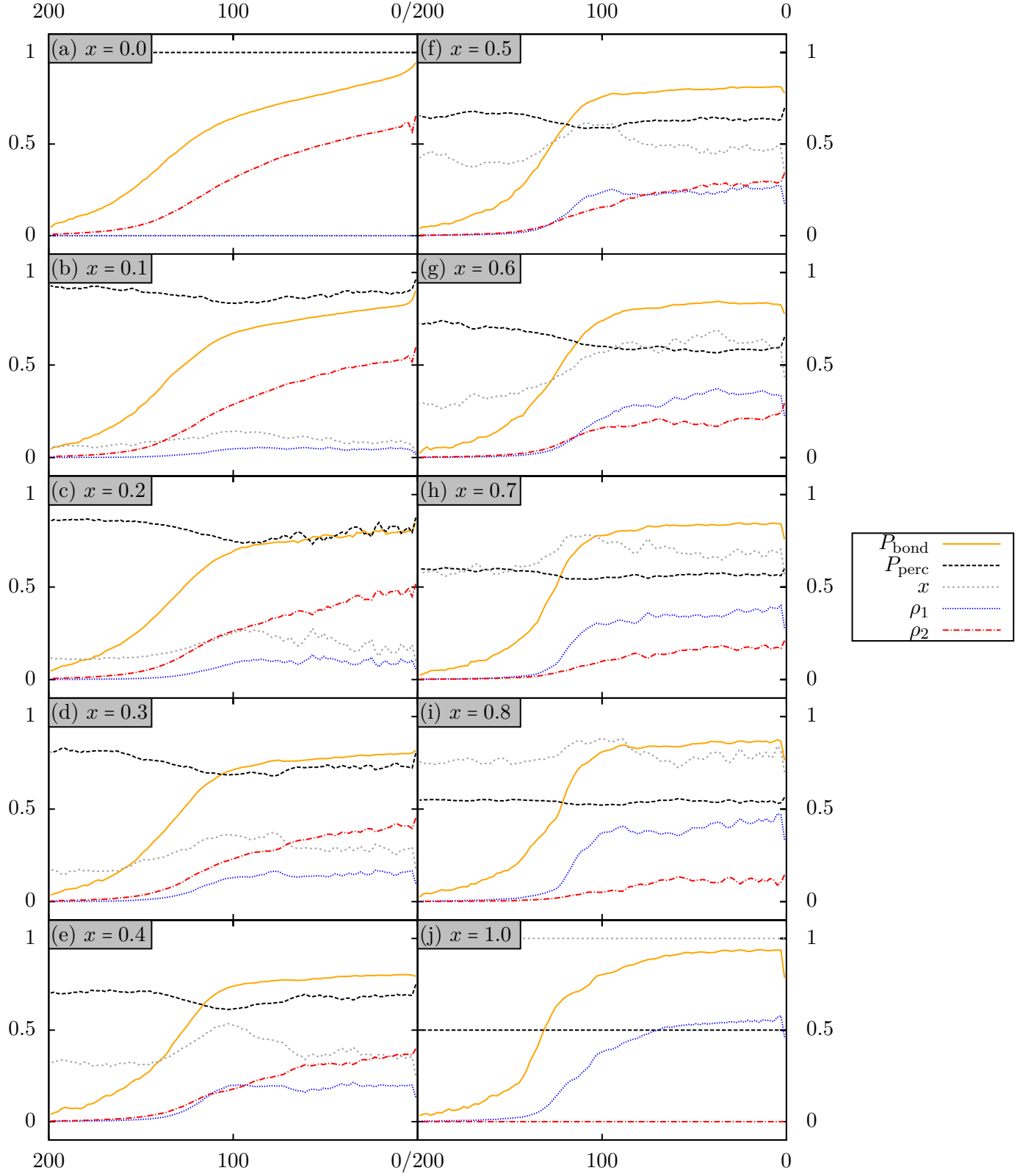


Figure 6: Bonding probability  $P_{\text{bond}}$ , percolation threshold  $P_{\text{perc}}$ , local composition  $x$ , species 1 packing fraction  $\rho_1$ , species 2 packing fraction  $\rho_2$  for different global compositions. Systems are percolated in regions where  $P_{\text{bond}} > P_{\text{perc}}$

### 3 Results

---

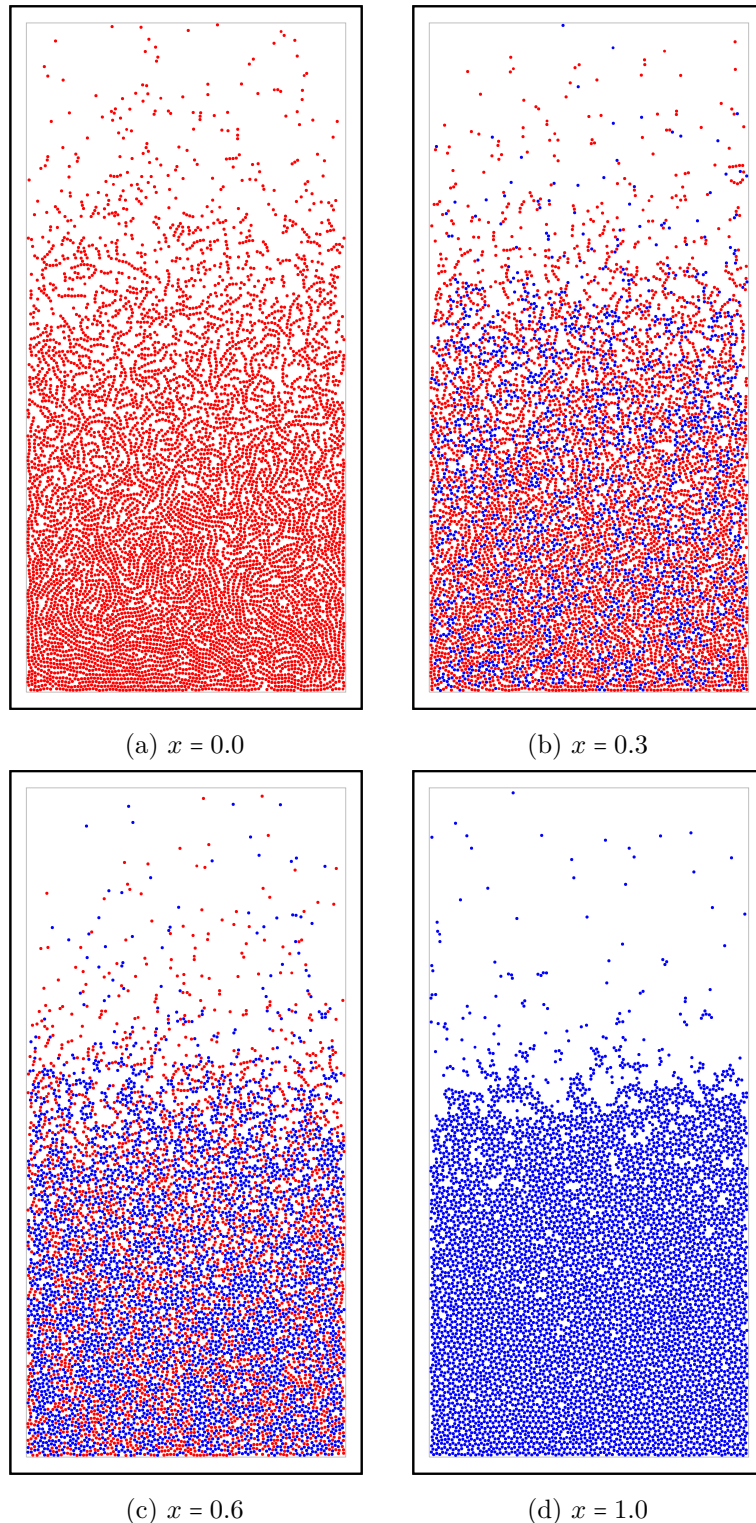


Figure 7: Final configuration for selected compositions as indicated. All boxes have a geometry of 100 by 200  $\sigma$ .

#### 3.1.3 Mixtures

As previously established, a pure system of species 2 (red dots) cannot percolate. On the other side of the spectrum, a pure system of species 1 (blue triangles) percolates easily. But how many species 1 particles do we need to get a (partially) percolated system? We see in figure 6c that for a composition of 0.2, the bonding probability barely reaches the percolation threshold. For higher compositions, a percolated state can always be observed, taking up at least half the box. „The higher the composition, the larger the percolated area“ seems to be a general rule, but we could not determine a concrete functional relation.

It is interesting to see that the bonding probability is quite even over the lower half of the box for mixtures with a medium composition (0.4 to 0.8) but if one species or the other dominates, it is sloped everywhere. This could indicate a homogeneous phase that only exists in a certain interval of the composition.

The stacking sequence (order of different phases in the box) is always the same: A high density phase at the bottom, and a low density phase on top.

#### 3.2 Varying the Ratio of Buoyant Masses

Next, we want to study the effect of different buoyant masses. The mass of species 1 (blue triangle),  $m_1$  is fixed as the unit of mass. We vary the relative mass of species 2 (red dot). Tested values for  $M$  were 6, 5, 4, 3, 2, 1, 0.5, 0.2, 0.1, -0.1, -0.2, -0.5, -1, -2, -3. We choose a composition of 0.6 and a temperature  $T^* = 0.15$ . The number of particles is 7500 and the simulation time  $3 \cdot 10^7$  MC steps.

##### 3.2.1 Negative Masses

If the buoyant masses of the species have opposite sign (in this case,  $m_2 < 0$ ,  $m_1 > 0$ ), the sedimentation path possesses a negative slope and thus can cross the binodal twice. We then expect three phases: Two high density phases with a low density phase in between. We can see just that for  $M$  between -3 and -1.0. When the relative mass gets closer to zero, the middle phase slowly vanishes as species 2 (red dot) particles fill the gap. At the same time, the percolated area gets bigger (see table 2).

Table 2: Size of percolated phase

$M:$	-3.0	-2.0	-1.0	-0.5	-0.2	-0.1
$P_{\text{bond}} = P_{\text{perc}}$ at $z/\sigma =$	70	70	72	76	82	86

On the other hand, the theory also predicts that both the top and bottom phase are percolated. This is clearly not the case, even though the bonding probability rises again after a steep dip at the lower liquid-gas interface. This could be an effect that disappears at lower temperatures, when more species 1 (blue triangle) particles are „trapped“ by species 2 (red dot) particles and enable the formation of a network.

### 3 Results

---

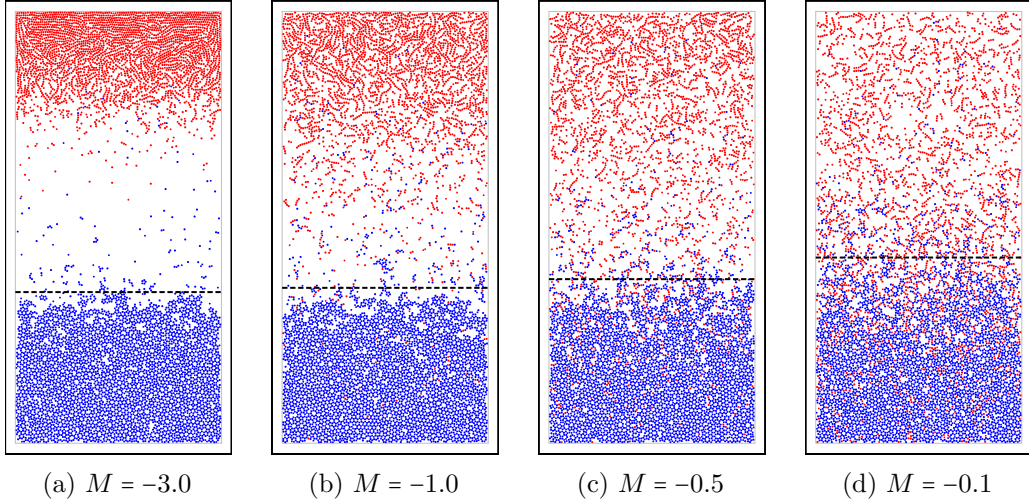


Figure 8: Final configurations for selected negative relative masses.  
Black dashed line in configurations indicates where  $P_{\text{bond}}$  cuts  $P_{\text{perc}}$ .

Again it can be observed that species 2  $\blacksquare$  has a much smoother liquid-gas interface than species 1  $\blacktriangle$ .

#### 3.2.2 Positive Masses

Starting at  $M = 0.1$ , we can see a direct continuation of the behaviour for low absolute negative masses. For  $M = \pm 0.1$ , the sign does not matter anymore, because thermal fluctuations and the bonding energy dictate the dynamics for species 2  $\blacksquare$ . This can be seen by comparing both the final configuration pictures and the respective plots.

Increasing the mass first empties the vapour phase. The packing fraction decreases from about 0.1 ( $M = 0.1$ ) to 0.01 and lower. At the same time, the distribution of species 2  $\blacksquare$  changes from mainly above species 1  $\blacktriangle$  to mainly below it. This happens when species 2  $\blacksquare$  becomes heavier than species 1  $\blacktriangle$ . Notice how at  $M = 1.0$  the densities are nearly the same, sans a scaling factor and some noise. The situation is much different already at  $M = 2.0$ . Instead of a density decreasing monotonically with height, species 1  $\blacktriangle$  now has a maximum density shortly below  $z = 100\sigma$  while species 2  $\blacksquare$  is most dense at  $z \rightarrow 0$ . This becomes only more prominent with further increasing  $M$ . At  $M = 3.0$  we begin to notice the same chains of species 2  $\blacksquare$  near the bottom of the vessel that we saw for the pure system. At  $M = 4.0$  the configuration approaches hexagonal packing in this area with some defects caused by species 1  $\blacktriangle$  particles.

This new phase not only has a very high density, but also shows some interesting properties in the bonding profile. The bonding probability nestles up against the percolation threshold, neither surpassing it noticeably nor falling under it. Only when the population of species 1  $\blacktriangle$  starts to rise, the bonding probability detaches from the percolation threshold and approaches a plateau before falling off again at the liquid-vapour phase boundary.

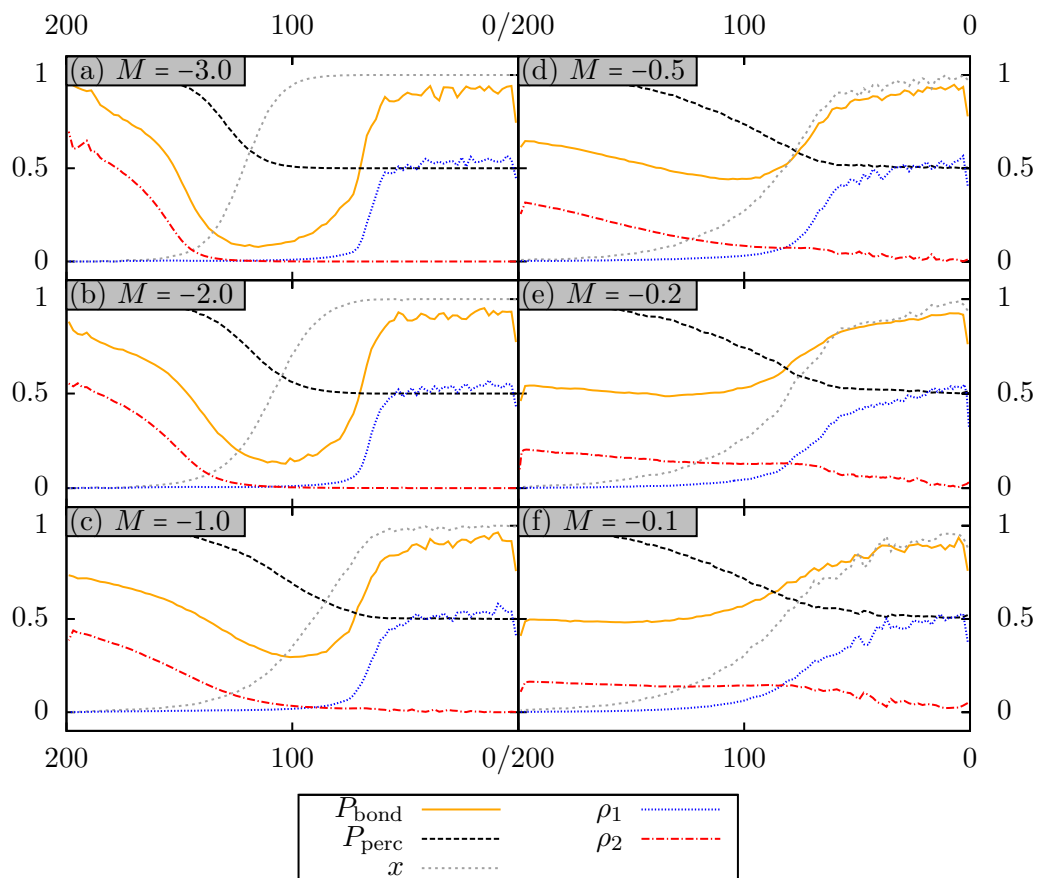


Figure 9: Bonding and packing fraction profiles for negative relative masses.

### 3 Results

---

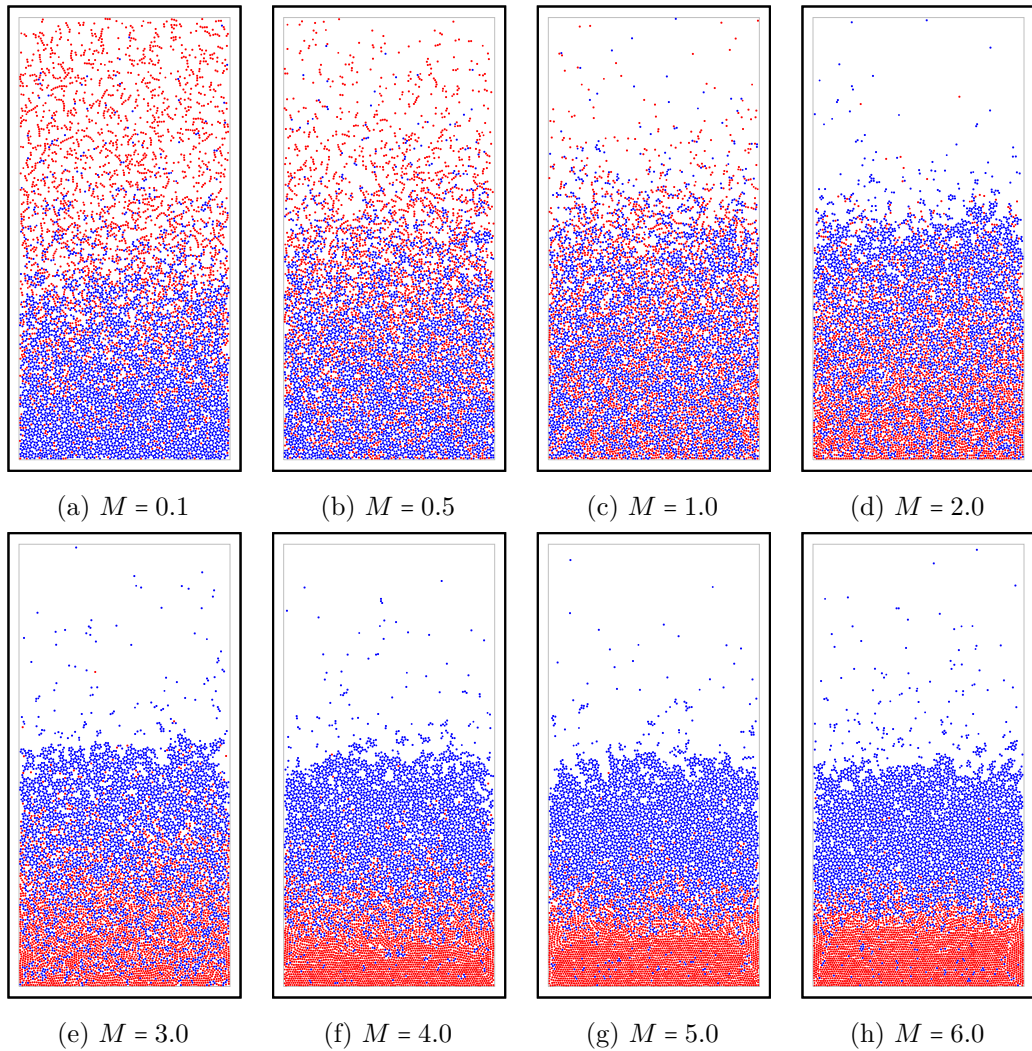


Figure 10: Final configuration for different relative masses ( $M$ ). All boxes have a geometry of 100 by 200  $\sigma$ .

### 3 Results

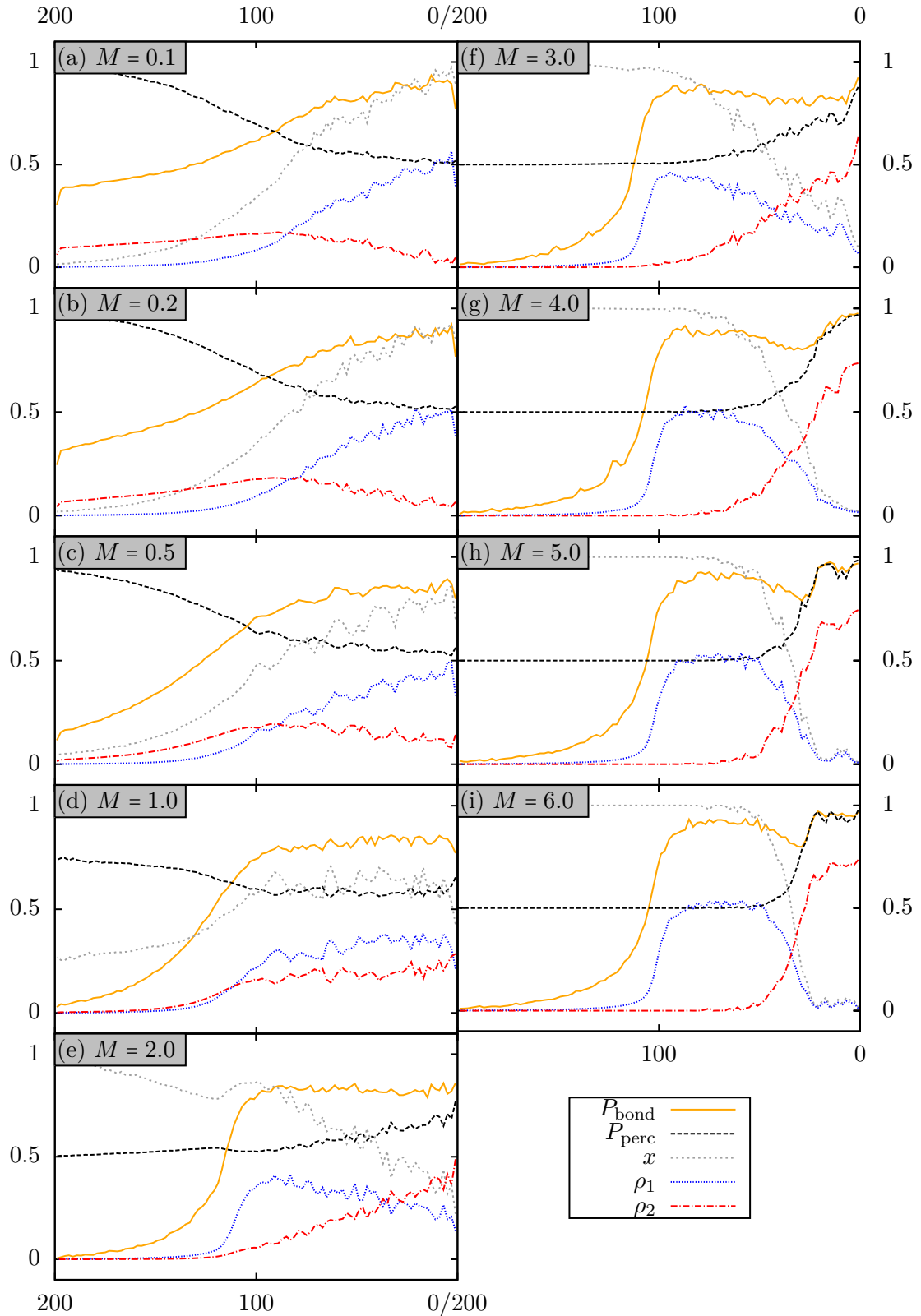


Figure 11: Bonding probability  $P_{\text{bond}}$ , percolation threshold  $P_{\text{perc}}$ , local composition  $x$ , species 1 packing fraction  $\rho_1$  and species 2 packing fraction  $\rho_2$ .  
Systems are percolated if  $P_{\text{bond}} > P_{\text{perc}}$

## 4 Conclusion and Outlook

In this thesis, we could reproduce the theoretically predicted phase sequences on the sedimentation path for a binary mixture of patchy colloids under gravity. We have shown that already a simple binary mixture with one kind of interaction shows rich phenomena that can be studied via a fairly straight-forward simulation approach. At the same time, the limitations of this approach became clear: Low temperatures require more sophisticated algorithms that increase the efficiency and avoid kinetic traps as described by Whitelam et al. [4]. A possible candidate is the Virtual Move Monte Carlo algorithm.

We established that a mixture can percolate with a low portion of species 1  particles ( $x = 0.3$ ) but does so more easily when the composition is higher (lower density required for a percolated phase). Simulations at high relative masses have shown an unexpected new phase of species 2  particles and a few species 1  particles. It shows a bonding probability right at the percolation threshold and a high density (near hexagonal packing). The properties of this phase and an explanation of the peculiar behaviour of the bonding probability have not been studied any closer. The possibility of a phase transition into a crystalline phase remains speculative without further examination.

Another aspect that has not been covered in this thesis are the transient network properties of these mixtures. We could see in the trajectory files that the network is constantly changing at a temperature  $T^* = 0.15$  while the macroscopic properties of the phases remained constant.

The software written for these simulations can easily be extended to study different parameter sets or different kinds of mixtures. It is fully documented (description of parameters, return values and purpose of every function is described) to make it easy to understand for people besides the author. To give access to anyone interested in building upon the work of this thesis, the source code is made publicly available via GitHub<sup>2</sup> at <https://github.com/mithodin/patchyColloids2014>.

---

<sup>2</sup><https://github.com/mithodin/patchyColloids2014>

## 5 References

- [1] E. Bianchi, J. Largo, P. Tartaglia, E. Zaccarelli, and F. Sciortino. ‘Phase Diagram of Patchy Colloids: Towards Empty Liquids’. In: *Physical Review Letters* 97.16 (2006), p. 168301. DOI: 10.1103/PhysRevLett.97.168301.
- [2] J. Russo, P. Tartaglia, and F. Sciortino. ‘Association of limited valence patchy particles in two dimensions’. In: *Soft Matter* 6.17 (2010), pp. 4229–4236. DOI: 10.1039/COSM00091D.
- [3] D. d. l. Heras and M. Schmidt. ‘The phase stacking diagram of colloidal mixtures under gravity’. In: *Soft Matter* 9.36 (2013), pp. 8636–8641. DOI: 10.1039/C3SM51491A.
- [4] S. Whitelam and P. L. Geissler. ‘Avoiding unphysical kinetic traps in Monte Carlo simulations of strongly attractive particles’. In: *The Journal of Chemical Physics* 127.15, 154101 (2007). DOI: 10.1063/1.2790421.
- [5] L. Rovigatti, D. de las Heras, J. M. Tavares, M. M. Telo da Gama, and F. Sciortino. ‘Computing the phase diagram of binary mixtures: A patchy particle case study’. In: *The Journal of Chemical Physics* 138.16 (2013). DOI: 10.1063/1.4802026.
- [6] D. de las Heras, J. M. Tavares, and M. M. Telo da Gama. ‘Phase diagrams of binary mixtures of patchy colloids with distinct numbers of patches: the network fluid regime’. In: *Soft Matter* 7.12 (2011), pp. 5615–5626. DOI: 10.1039/COSM01493A.
- [7] D. de las Heras, N. Doshi, T. Cosgrove, J. Phipps, D. I. Gittins, J. S. van Duijneveldt, and M. Schmidt. ‘Floating nematic phase in colloidal platelet-sphere mixtures’. In: *Scientific Reports* 2 (2012). DOI: 10.1038/srep00789.
- [8] B. Widom. ‘Some Topics in the Theory of Fluids’. In: *The Journal of Chemical Physics* 39.11 (1963), pp. 2808–2812. DOI: 10.1063/1.1734110.
- [9] M. Lindner. *libconfig - C/C++ Configuration File Library*. July 9, 2014. URL: <http://www.hyperrealm.com/libconfig/>.

## 6 APPENDIX A: Implementation Details

The implementation was done in C using only the standard libraries, and libconfig [9] to load the configuration file. An automatic build file is provided for use with CMake<sup>3</sup>. Documentation can be built using Doxygen<sup>4</sup>. In the following paragraphs, I will shortly highlight a few details of the implementation.

The values for  $d_{\max}$  and  $\alpha_{\max}$  (the maximum trial displacement and rotation) are chosen at the beginning of the simulation in iterations of 4000 MC steps each. We alternately multiply  $d_{\max}$  and  $\alpha_{\max}$  by the average acceptance rate of the iteration over the desired acceptance rate  $\frac{p_{\text{avg}}}{p_{\text{desired}}}$ <sup>5</sup>. For the runs where  $\alpha_{\max}$  is going to be updated,  $d_{\max}$  is temporarily set to 0. [*monte\_carlo.c, initDmax()*]

To get the desired acceptance rate even when there are lots of bonds, we repeat this process until the total energy of the system for the last iteration divided by the average over the previous 10 is different from one by no more than  $5 \cdot 10^{-3}$ , so the system is already near equilibrium. When this criterion is met, we continue to iterate until the acceptance rate for the latest iteration does not differ from the desired one by more than 1%.  $d_{\max}$  and  $\alpha_{\max}$  are then fixed and the proper simulation is started.

The information about each colloid is stored in a **struct** that contains (among other things) its coordinates  $x_i$ ,  $z_i$ ,  $\alpha_i$  as well as its species and a pointer to the colloid above and below the current one, going by the value of the  $z$  coordinate. We thus get a doubly linked ordered list of all colloids that we can use to get a reduced set of possible interaction partners by iterating (in both directions from the current one) over the list up to the first colloid whose  $z$  coordinate differs by more than  $\delta + \sigma$  from the current one's<sup>6</sup>. [*monte\_carlo.c, pairPotential()*] The cost is that the list has to be re-sorted for each trial move of a particle *before* the new energies are being calculated, and then updated again iff the move is rejected. Apart from that, the code is designed in a way that makes rejecting a move as (computationally) cheap as possible, because the number of rejected moves exceeds that of accepted moves.

We also store an array of the current bonding partners and the current external and internal energy to simplify calculating the change in energy for a trial move. Both have to be updated once a move has been accepted.

The parameters of the simulation are provided in a configuration file and loaded using libconfig [9] [*load\_config.c*]. The configuration file format allows for arrays of parameters to be given. The program will then run all combinations of these parameters. Multiple parameter sets can be simulated in parallel. The maximum number of concurrent simulations has to be passed to the program as a command line argument and defaults to 1. The program also supports loading the initial configuration of the simulation from

<sup>3</sup><http://www.cmake.org>

<sup>4</sup><http://www.stack.nl/~dimitri/doxygen/index.html>

<sup>5</sup>This gives an inversely linear approximation of the function  $p_{\text{accept}}(d_{\max}, \alpha_{\max})$

<sup>6</sup>assuming a uniform density, we can in this way reduce the number of possible interaction partners by a factor of  $\frac{200}{2(\delta+\sigma)} \approx 90$

a file specified in `parameters.cfg`. If this is the case, the thermalisation is skipped.

### 6.1 Data

The simulation exports different files containing data about the state of the simulation.

- In `positions-<identifier>.dat`, the coordinates of all the colloids in the final configuration are stored. From it, we can generate images to analyse the phases visually. We can also use this file as an initial state for a new simulation.
- In `movie-<identifier>.xyz`, we store the x and z coordinates of all the colloids in a regular interval throughout the simulation. From it, we can generate a movie of the sedimentation process as well as density profiles over time. The data format is readable by the University of Illinois' VMD<sup>7</sup>.
- In `statistics-<identifier>.dat`, we store the density profile and the bond saturation (see 2.3) averaged over the whole simulation, separated by species.
- In `energy-<identifier>.dat`, we store the internal, external and total energy every few MC steps. We can use this data to find out whether the system has reached an equilibrium state or not.

`<identifier>` is a string signifying the parameter set used by the simulation.

### 6.2 Analysis tools

We wrote multiple tools to further analyse the simulation output. For easy tasks, we used Python and C for tasks that required speed.

- `density_time.py` Takes a movie file and a number  $N$ . Creates a new file with density profiles averaged over  $N$  movie frames<sup>8</sup>.
- `radial_paths.py` Takes a final configuration file. Creates a histogram of the number of connected particles over the total number of particles as a function of the distance from a pivot particle<sup>9</sup>. Particle  $i$  and  $j$  count as *connected* when either there exists a particle  $\zeta$  that has a direct bond with particle  $i$  and is connected to  $j$ , or  $i$  is directly bonded with  $j$ .
- `radial_distribution_function.c` Calculates the radial distribution (pair correlation function), averaged over multiple frames, from a movie file.
- `perc_threshold.c` Calculates the percolation threshold and bonding probability, averaged over multiple frames, from a movie file.

---

<sup>7</sup><http://www.ks.uiuc.edu/Research/vmd/>

<sup>8</sup>one frame consists of the coordinates of all colloids at a given Monte Carlo step

<sup>9</sup>averaging over all particles

## **Erklärung**

Hiermit bestätige ich, dass ich die vorliegende Arbeit selbst verfasst, nur die angegebene Literatur als Hilfsmittel verwendet habe und alle wörtlich oder sinngemäß übernommenen Äußerungen anderer Autoren gekennzeichnet habe. Außerdem versichere ich, dass ich die Arbeit zu keinem früheren Zeitpunkt bereits zur Erlangung eines akademischen Grades eingereicht habe.

Bayreuth, August 18, 2014

---

Lucas Treffenstädt